International Journal of Dynamics and Control (2026) 14:199
https://doi.org/10.1007/s40435-026-02134-w

RESEARCH

Design, control and implementation of AI-driven autonomous snake robot for archeological site exploration

Mohamed Shehata[1] · Ahmed Elsayed[1] · Ibrahim Saeed[1] · Ahmed Yones[1] · Mohamed Salem[1]

Received: 11 February 2026 / Revised: 2 April 2026 / Accepted: 21 April 2026

Abstract

For decades, archeological site exploration has presented major challenges due to narrow spaces, unstable structures, and the high sensitivity of historical artifacts. Recent advancements in robotic technologies have introduced highly capable and reliable alternatives for safe and efficient exploration in environments that are otherwise inaccessible or hazardous to humans. This paper presents mathematical modeling, design, control and implementation of a bio-inspired autonomous snake robot tailored for the exploration of confined environments, with a particular focus on archeological sites. Our primary contribution is a novel system integration approach designed specifically for highly confined and fragile heritage environments, successfully combining a modular alternating-joint architecture with a ROS-based control framework and an AI-driven perception system focused strictly on YOLOv11-based artifact and obstacle identification. A physical network model was developed using MATLAB Simscape to simulate the system dynamic behavior under varying payloads. The control architecture was implemented using the robot operating system (ROS), supporting real-time execution of multiple locomotion strategies through coordinated servo actuation. The system is validated through simulation and physical experiments, demonstrating stable undulatory locomotion, accurate mapping in confined environments, and reliable artifact detection under variable lighting and occlusion. The results indicate that snake-inspired robotic platforms provide a viable and scalable solution for autonomous exploration and documentation in sensitive heritage sites.

Keywords Snake robot · Heritage sites · Archeological exploration · Bio-inspired

1 Introduction

Archeological sites are rich repositories of human history, providing key insights into the cultural, social, and technological development of ancient civilizations. Yet, most sites present considerable challenges to traditional exploration due to physical limitations [1]. Confined corridors, unstable structures, and fragile artifacts routinely exclude direct human access, while environmental factors like dust, debris, and limited lighting create additional hazards to personnel safety [2]. These constraints highlight the necessity for non-invasive, high-resolution exploration methods that maintain site integrity while facilitating detailed documentation [3, 4]. The integration of robotic systems in archeological settings has become an encouraging response to these issues. Such robots offer consistent and minimally invasive means of accessing dangerous or difficult-to-reach locations. Representative applications include autonomous site mapping, artifact documentation, and reconnaissance operations in subsurface or underwater settings [5, 6]. Endowed with sophisticated perceptual and sensing abilities, robotic platforms can acquire extensive spatial information, track site conditions over long periods, and greatly minimize the necessity of intrusive human involvement.

One notable precedent in archeological robotics is the (Djedi) project, which employed a custom-built wheeled robot to explore narrow shafts branching from the Queen's

✉ Mohamed Shehata
mohamed.saleh@bhit.bu.edu.eg

Ahmed Elsayed
ahmed20375@beng.bu.edu.eg

Ibrahim Saeed
Ibrahim.saidesci@ieee-bub.org

Ahmed Yones
ahmed191021@beng.bu.edu.eg

Mohamed Salem
mohamed.eltaher@bhit.bu.edu.eg

[1] Department of Mechanical Engineering, Benha Faculty of Engineering, Benha University, Banhā, Egypt

Published online: 21 May 2026

Chamber in the Great Pyramid of Giza [7, 8]. The robot used an inchworm-like locomotion mechanism and was equipped with bespoke instruments like a micro-snake camera and precision drill, making it possible to examine in detail fragile, previously inaccessible passages. Created through the cooperation of global experts and led by the University of Leeds, the system prioritized minimal structural disruption to preserve the monument's integrity during exploration. The successes of the (Djedi) project demonstrated the feasibility of robotic, non-invasive archeological investigation in highly restricted heritage environments and encouraged further investigations into flexible, snake-like robotic platforms [9]. Despite their functional benefits, wheeled platforms, such as those used in the (Djedi) project, face severe limitations when deployed in settings characterized by irregular terrain, heavy debris, or extremely narrow passages. Other highly relevant approaches in archeological robotics include tracked, wheeled-legged, and hexapod systems. For instance, Wang et al. proposed a modular robotic system for exploration [10], while Shao et al. demonstrated the efficacy of articulated hexapod robots (A-RHex) for archeological pre-exploration [11]. While hexapod and tracked systems offer excellent mobility over rough terrain, they are physically constrained by their bulk. In contrast, an undulating snake morphology is uniquely capable of penetrating ultra-narrow, low-clearance shafts–such as the 20×20 cm air shafts found in the Great Pyramid–that leg-based systems cannot physically enter. Consequently, robots derived from serpentine locomotion enable enhanced mobility in these highly restricted situations [12]. Their articulated body allows for different modes of movement, such as serpentine, sidewinder, and concertina motions, which enable passage through narrow apertures, over objects, and along irregular terrains [13].

Recent developments in snake robot technology have radically enhanced their applicability to archeological and other confined-space applications [14]. Advances in mechanical design, actuation, control algorithms, and power-efficient locomotion have resulted in platforms that are more stable, versatile, and able to operate for extended periods. In addition, the development of deep learning-based perception systems and 3D spatial mapping has allowed these robots to identify, classify, and move toward zones of archeological interest in complicated and unstructured environments [15]. In our proposed system, we implement an AI-driven approach specifically localized to the visual perception module; by utilizing YOLOv11 for real-time artifact detection and spatial reasoning, the robot achieves a level of autonomous environmental awareness, even though the low-level locomotion and path execution remain reliant on robust kinematic controllers. The article is organized as follows: introduction, computational work including the software used for modeling, design, and control, followed by experimental work and the method of manufacturing and assembling the robot parts, and finally, the results and discussion.

2 Computational work

The snake robot system was comprehensively modeled using MATLAB Simscape to achieve accurate representation of the multibody system dynamics and control interactions [16]. The modeling approach integrated mechanical components, electrical systems, and control algorithms within a unified simulation environment, enabling detailed analysis of locomotion patterns and system performance before physical implementation [17, 18]. Figure 1 illustrates the complete modeling and simulation work flow adopted for the snake robot development process.

The Simscape environment provided significant advantages for this application through its multi-domain simulation capability that integrates mechanical and electrical subsystems, automated equation generation from physical component connections, real-time visualization of robot motion and contact forces, seamless integration with MATLAB control design tools, and efficient computation of complex multibody dynamics [19].

2.1 Mechanical system architecture

The mechanical structure comprises an articulated chain-link structure of 12 cylindrical segments with alternating orthogonal joints driven by servo motors. This configuration provides the fundamental framework for three-dimensional serpentine movement. The complete system architecture integrates these mechanical components, sensing systems, actuation blocks, and locomotion pattern generators within the Simscape environment to create a comprehensive simulation platform [20]. As demonstrated in Fig. 2, the system architecture incorporates several key subsystems that work in coordination to achieve the desired locomotion capabilities. The mechanical structure comprises 12 cylindrical body segments with alternating joint configuration that provides the fundamental framework for movement.

The actuation system utilizes servo motor blocks with position control and torque limiting to ensure precise joint control while preventing mechanical damage [21]. The sensing framework incorporates joint angle, velocity, and torque measurement systems that provide essential feedback for closed-loop control. The control interface manages pattern generation and mode switching mechanisms to enable different locomotion strategies. Finally, the environment model simulates ground contact and friction forces to provide realistic interaction dynamics. Each body segment was modeled as a rigid cylindrical body with specific mass and inertial properties derived from the CAD design, as shown in Fig. 3.

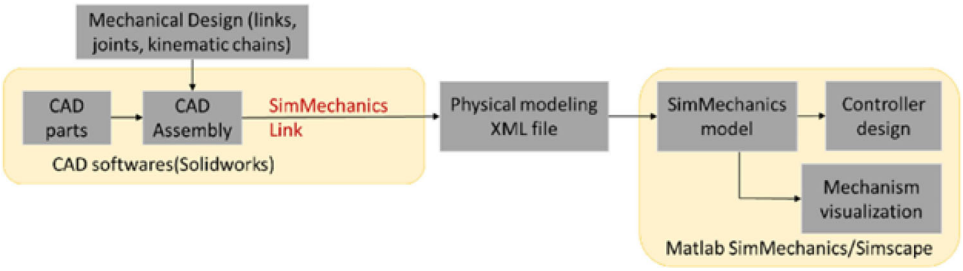

Fig. 1 Snake robot modeling and simulation workflow

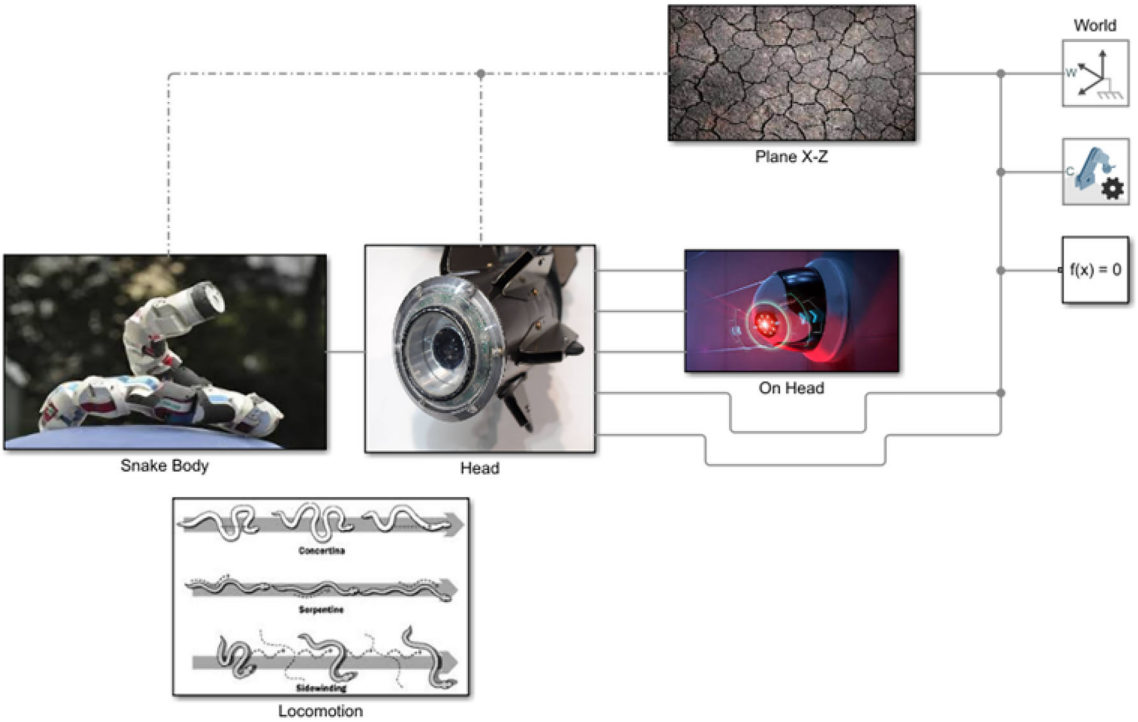

Fig. 2 Complete system architecture of snake robot simulation model

Fig. 3 CAD model of joint configuration

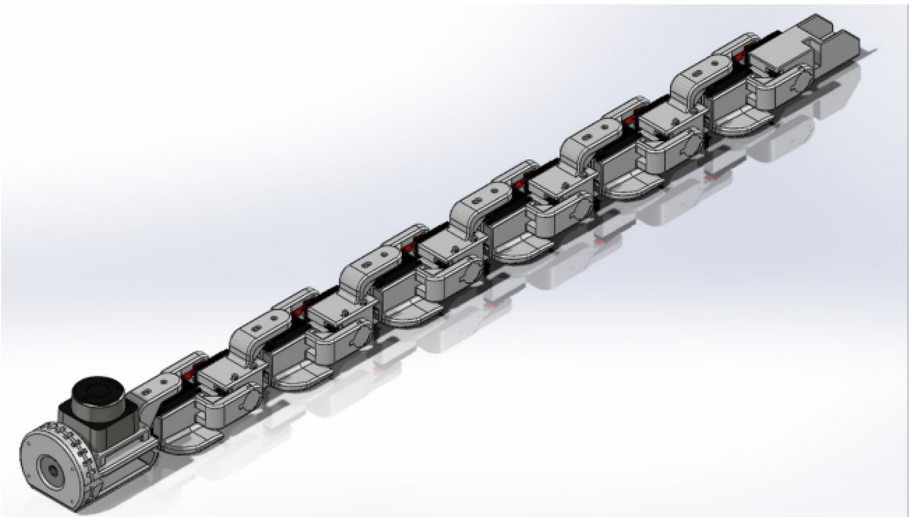

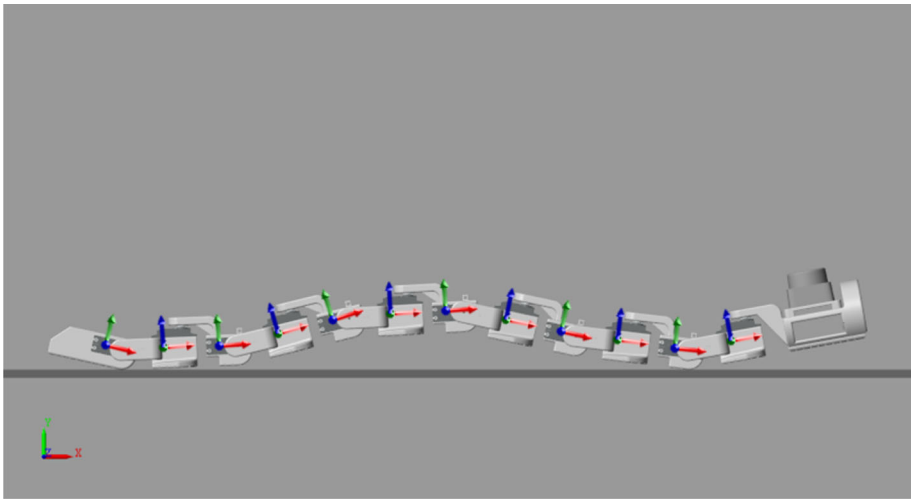

Fig. 4 Individual segment design and joint configuration

The system components were carefully designed to balance functionality with weight constraints. The body segments, each weighing 80 grams, serve as the primary structural elements with 12 total segments comprising the complete robot structure. Joint actuators weighing 40 grams each provide rotational actuation for the 12 interconnection points between segments. The head module, at 150 grams, functions as the sensor mounting platform and houses the primary navigation and sensing equipment. The electronics housing, weighing 60 grams, provides control system integration and protects the computational components from environmental factors. The alternating joint configuration represents a critical design decision that enables three-dimensional locomotion while maintaining mechanical simplicity. The system incorporates 6 joints operating in the X-Z plane to provide vertical undulation capabilities, complemented by 6 joints operating in the X-Y plane for horizontal undulation. Each joint maintains an angular range of ± 90 degrees, providing substantial flexibility for complex motion patterns. The maximum angular velocity of 180 degrees per second ensures rapid response to control commands, while the maximum torque capacity of 2.5 N·m provides sufficient force generation for locomotion across various terrain conditions.

2.2 Simulation-based dynamic modeling

Given the high degrees of freedom and the complex, nonlinear ground interactions inherent to snake robot locomotion, deriving an analytical dynamic model (e.g., using Lagrangian mechanics) becomes computationally restrictive and prone to idealization errors. Therefore, in this work, the dynamic analysis was formulated computationally utilizing the MATLAB Simscape Multibody environment. This simulation-driven approach allowed for a highly accurate representation of the physical prototype under operational conditions. The dynamic model was constructed by importing the precise 3D CAD geometry of the robot's links. The software automatically computed the inertia tensors and center of mass for each distributed segment. Crucially, the dynamic simulation incorporated the environmental interaction models necessary for bio-inspired locomotion:

- **Joint dynamics:** Actuator constraints were modeled by applying realistic internal friction and damping coefficients to the alternating pitch and yaw revolute joints.
- **Contact mechanics:** The Spatial Contact Force block in Simscape was utilized to model the normal forces and the anisotropic Coulomb friction between the robot's cylindrical body segments and the ground surface. This friction asymmetry is the fundamental mechanism that propels the robot forward during undulation.

Instead of classical analytical derivation, the system dynamics were analyzed using MATLAB Simscape Multibody [22]. The CAD assembly was imported to preserve the exact mass and inertia tensor properties of the custom 3D-printed components. The linear motion is modeled using Prismatic Joint blocks with assigned internal mechanics parameters to represent the friction of the linear bearings. Figure 4 follows an alternating pattern to provide three-dimensional locomotion capabilities while maintaining mechanical simplicity and manufacturing feasibility [23].

The mechanical and electrical subsystems of the snake robot were modeled using MATLAB Simscape to achieve accurate and dynamic representation of the physical behaviors. Simscape simulation environment enabled the integration of mechanical components such as joints, links, and actuators with electrical elements including motors, sensors, and power electronics [24]. This modeling approach facilitated detailed analysis of actuator dynamics, torque requirements, and sensor feedback under realistic operating conditions. The use of Simscape allowed for validation of

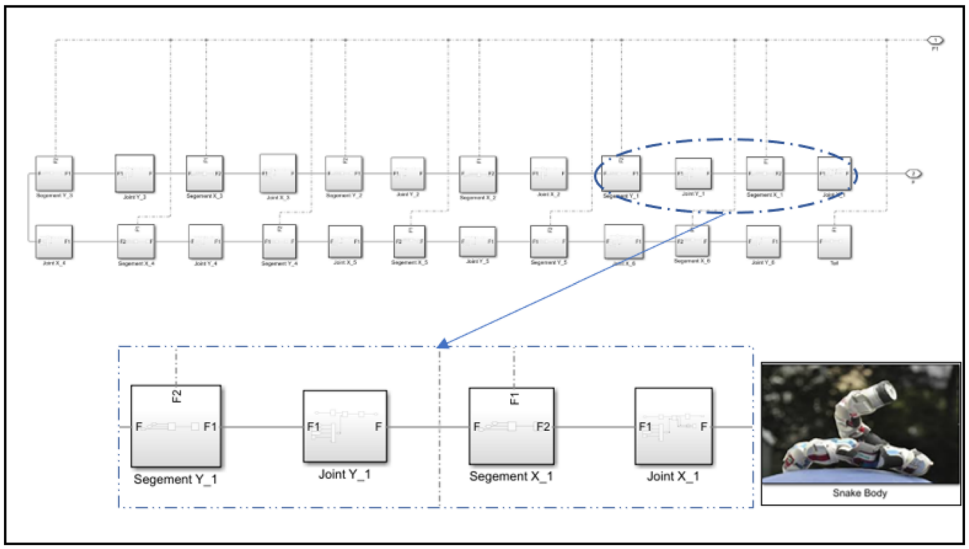

Fig. 5 Alternating joint configuration diagram

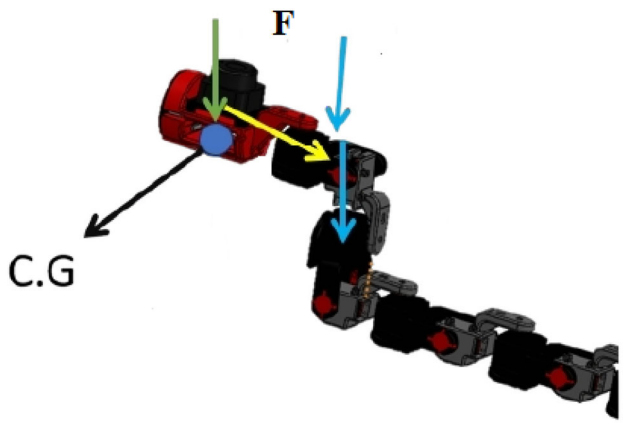

Fig. 6 Worst structure position for snake robot configuration

mechanical designs and electrical control strategies before physical implementation, thereby reducing prototyping risks and optimizing system performance. The joints are actuated by motion inputs simulating the stepper motor profiles, allowing for the verification of torque requirements during the acceleration phases of the retrieval cycle, see Fig. 5.

The snake robot consists of 12 identical cylindrical segments connected by alternating joints operating in orthogonal planes. Each segment has a length of 0.1 m and a diameter of 0.05 m. While the bare 3D-printed shell of a single segment weighs 80 grams. The lumped mass used for Simscape Multibody dynamic modeling is 0.2 kg. This accounts for the fully assembled segment, the 40 g servo motor, internal wiring, fasteners, and a dynamic safety margin. The robot was placed in its worst position to calculate the forces acting on the links and use them in the design, see Fig. 6.

The MATLAB Simscape modeling served as an essential predictive tool to calculate the peak dynamic torque requirements under the worst-case payload configurations.

Table 1 Physical contact and joint dynamics parameters

Parameter	Value	Unit
Static friction coefficient (μ_s)	[0.5]	–
Kinetic friction coefficient (μ_k)	[0.3]	–
Contact stiffness (k)	[10^6]	N/m
Contact damping (c)	[10^3]	N·s/m
Transition region width	[10^-4]	m
Critical velocity	[10^-3]	m/s

Table 2 Simscape simulation environment configurations

Configuration parameter	Setting
Solver type	[e.g., ode23t (Mod. stiff)]
Max step size	[e.g., Auto / 0.01 s]
Contact force sensing	Enabled
Joint actuator mode	Provided by input
Motion sensing	Enabled

Each joint incorporates a comprehensive actuation subsystem implemented through Simscape component blocks that provide detailed modeling of the electromechanical interactions. The joint control architecture includes position feedback, torque limiting, and sensor integration to create a robust and reliable actuation system as demonstrated in Table 1 for physical dynamic parameters and Table 2 for Simscape simulation parameters.

Simscape simulations indicated a maximum joint actuation torque of 0.4 N·m, as shown in Fig. 7. This predictive step directly dictated our selection of the FT5835M servo motors.

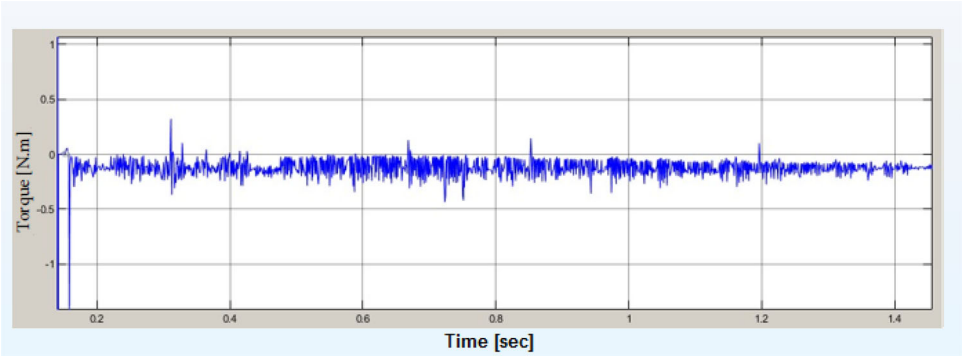

Fig. 7 Actuation torque output from Simscape simulation showing maximum torque

2.3 Robot structure design

The design and analysis of snake robot segments are essential for ensuring mechanical stability and flexibility across various terrains. CAD software such as SolidWorks is employed to create a detailed 3D model of the snake robot segment. Each segment is designed to be lightweight yet strong enough to withstand dynamic bending and torsional loads during motion. These design choices also enhance modularity and thermal dissipation, especially when motors are embedded inside the body. The model ensures compatibility between all segments and provides proper clearances for revolute joints, wiring paths, and mounting of internal components. The same segment design can be used repetitively to build a full body structure, maintaining uniform mechanical behavior throughout the robot. After evaluating the distinct characteristics of the three most common 3D printing materials PLA, ABS, and PETG a comparison of their relative advantages and disadvantages led to the selection of PETG for the snake robot fabrication due to its superior balance of mechanical strength and durability.PETG (Polyethylene Terephthalate Glycol) is a popular thermoplastic material widely used in robotic systems due to its excellent balance of strength, flexibility, and ease of manufacturing. In the context of snake robot design, PETG is particularly advantageous for fabricating body segments and enclosures that require moderate mechanical strength with low weight. Table 3 illustrate mechanical properties of PETG material used in the snake robot fabrication.

Based on mathematical modeling results, structural analysis was conducted using ANSYS software to evaluate the mechanical response of a snake robot body part when a motor-driven joint is actuated using the peak torque as the load case. The boundary conditions were designed to reflect the actual operational configuration of the robot. Specifically, the interface between the part and the integrated motor arm was selected as the region for force and torque application. The mesh was constructed primarily using tetrahedral solid elements to account for the complex geometry of the assembled segments and actuators. The relevance center was

Table 3 Material properties of PETG Material

Material properties	Value
Elastic modulus	2.2 GPa
Poisson's ratio	0.33
Shear modulus	470 MPa
Density	1290 kg/m^3
Tensile strength	53 MPa
Compressive strength	55 MPa
Yield strength	47.9 MPa

adjusted to Fine, and the mesh transition was set to Medium to balance computational cost with detail resolution. The results confirmed that the 3D-printed PETG structure operates safely within allowable stress and deformation limits, as illustrated in Fig. 8. Figure 8a shows that the maximum total deformation was found to be approximately 0.730 mm, occurring near the region where the force is applied. The stress distribution, illustrated that reveals a maximum von Mises stress of 60.124 MPa, which is safely below the tensile yield strength of PETG. This confirms that the structure remains within the elastic range under the applied loading conditions. The minimum predicted fatigue life was zero cycles in critical regions (indicating potential failure under high repetition), whereas the maximum was on the order of $1x10^6$ cycles, as shown in Fig. 8b .

2.4 ROS-based control and data flow

The control architecture of the snake robot is organized into hierarchical layers implemented in the Robot Operating System (ROS). At the highest level, perception and mapping modules process sensory data from LiDAR and onboard cameras to detect obstacles and estimate the robot pose. This information is forwarded to the motion planning module, which generates desired paths or shapes suitable for the articulated body [25]. The high-level control layer translates these paths into motor torques, while the low-level control layer computes the corresponding joint reference angles and trans-

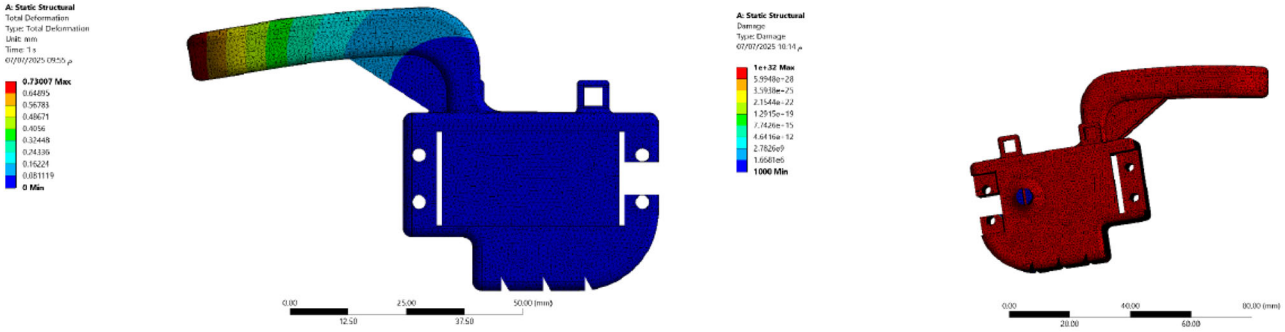

(a) Total Deformation for segment (b) Fatigue Damage

Fig. 8 ANSYS results under maximum torque load

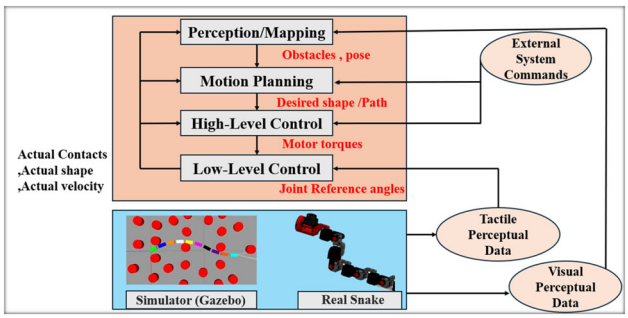

Fig. 9 Autonomous system architecture

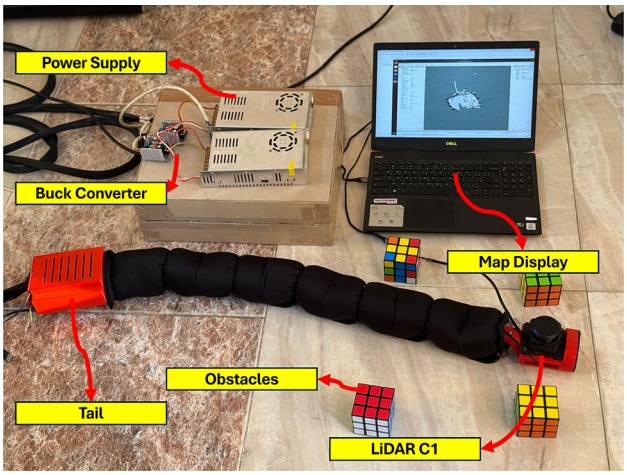

Fig. 10 ROS-based control and data flow architecture integrating perception, planning, and actuation across simulation and real hardware

mits them to the actuators. In practice, the ROS nodes running on the NVIDIA Jetson handle SLAM, obstacle detection, and locomotion planning in real time. Control commands are then sent via a serial link to an Arduino-based low-level controller, which generates the PWM signals required to drive the FT5835M servo motors [26]. Following the simulation phase, the ROS framework was deployed on the physical prototype to validate real-time sensing, mapping, and control, as shown in Fig. 9.

The architecture is designed to operate both in simulation (Gazebo) and on the physical prototype. In simulation, Gazebo provides joint states and contact dynamics, which ROS uses for perception and control testing. In the real robot, tactile and visual perceptual data are streamed from the sensors to the ROS nodes. This unified flow of sensing, processing, and actuation ensures seamless transition from simulation to real-world deployment, as illustrated in Fig. 10.

The LiDAR module was interfaced with ROS to publish range data on the scan topic, and the readings were visualized in RViz to confirm reliable detection of nearby obstacles and walls. These scans formed the raw input for subsequent mapping and navigation tasks. Using Hector SLAM, real-time occupancy grid maps were generated and continuously updated during operation. Because snake robots rely on deliberate slip to achieve serpentine locomotion, calculating odometry from joint encoders is highly unreliable. Hector SLAM mitigates this fundamental issue by bypassing odometry entirely, relying instead on high-frequency LiDAR scan-matching to estimate the robot's pose. Furthermore, navigating long, featureless, and repetitive ancient corridors can easily cause scan-matching algorithms to fail. To address this, we relied on the high update rate of the LiDAR to ensure sufficient overlap between consecutive scans, preventing the drift often seen in textureless archeological environments. The generated maps provided accurate representations of the environment and were stored for later analysis. This mapping capability enabled the robot to maintain awareness of obstacles and free space while navigating autonomously. The navigation process relied on a local analyzer node that processed the SLAM map together with the robot's pose to infer simple motion states. Depending on obstacle configurations detected within a 20 cm radius, the node generated commands such as forward, left, right, or avoidance maneuvers. These decisions formed the basis for motion planning in real-world conditions. Finally, the motion decisions were transmitted to

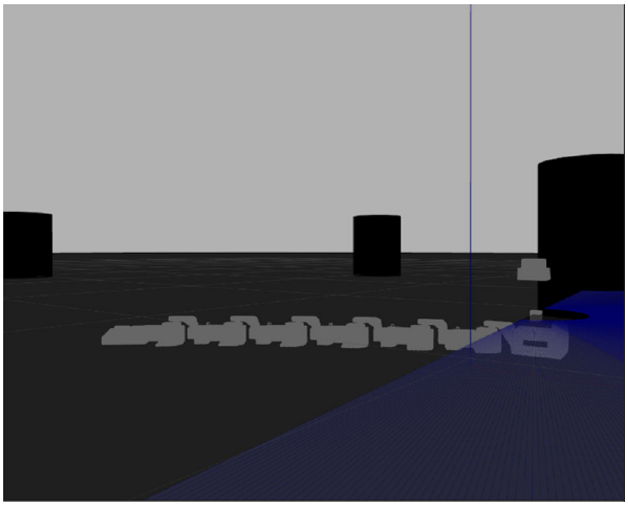

Fig. 11 Robot model in Gazebo

the Arduino microcontroller through a serial sender node. The Arduino converted the incoming commands into PWM signals that drove the FT5835M servo motors, executing the selected gait in real time. This closed the loop between sensing, decision-making, and actuation, enabling computationally autonomous navigation in the physical setup. The physical structure and configuration of the snake robot in the Gazebo simulation environment is illustrated in Fig. 11, where the segmented body and overall morphology are clearly visible.

2.5 AI model training and optimization

To enable autonomous archeological artifact exploration, an AI model built based on state-of-the-art YOLO architectures specialized for heritage detection scenarios. Object detection has experienced remarkable evolution, moving from early handcrafted feature-based methods to highly optimized deep learning frameworks. Conventional methods frequently did not adjust to the variety of artifact morphologies, variations in illumination, and partial occlusions that are typical in archeological settings [27]. Many of these restrictions were removed with the advent of deep learning, especially convolutional neural networks, which made it possible for scalable training on a variety of data sets and automatic feature extraction. Because of its single-stage detection pipeline that combines real-time localization and classification, the YOLO family has shown itself to be particularly effective among them. The most recent version, YOLOv11, ensures high precision and quick inference by introducing anchor-free detection, enhanced multi-scale feature fusion, and lightweight modules tailored for embedded systems [28]. This makes it a good fit for applications that need to be deployed on the go, such as snake robots used for autonomous archeological exploration. YOLOv11 provides a strong balance between accuracy, speed, and computing efficiency, adapting well to the recognition of cultural heritage artifacts through transfer learning and domain-specific data augmentation. As a result, it offers a workable way to detect heritage in real time, facilitating safe transit in constrained or delicate areas as well as recording and preservation. The architecture of YOLOv11 is composed of three core modules as illustrated in Fig. 12.

The backbone, which extracts discriminative features through optimized convolutional blocks; the Neck, which integrates multi-scale representations using Spatial Pyramid Pooling-Fast (SPPF) and C2f modules; and the head, which employs anchor-free detection to generate bounding boxes, class predictions, and confidence scores with enhanced loss functions [29]. In order to balance accuracy and computational economy, training is carried out on GPU-enabled settings with carefully adjusted hyperparameters, such as an Adam optimizer, a cosine-decayed learning rate, and an input resolution of 640×640 pixels. In order to ensure applicability to unknown archeological contexts, data augmentation and regularization further reduce overfitting. Lastly, the system is assessed using well-known metrics including precision, recall, mAP@0.5, and mAP@0.5:0.95, which offer a thorough understanding of both localization precision and classification accuracy. Through inference on previously unknown artifact photos, qualitative assessments are also carried out, showcasing the model's capacity for dependable real-time recognition and assisting with autonomous navigation and documentation tasks during heritage exploration [30]. A domain-specific dataset was constructed for archeological artifact recognition. Images were collected from institutional archives, public heritage repositories, and curate online datasets, resulting in a corpus exceeding 7,000 labeled images. The dataset includes representative artifact categories such as pottery, statues, inscriptions, and structural fragments. The dataset was split into training (70%), validation (20%), and testing (10%) subsets to ensure generalization.

3 Experimental work

The transition from conceptual design to a functional, field-ready prototype was achieved, as illustrated in Fig. 13, confirming the robot readiness for operation in real-world, constrained environments.

The snake robot supports various biologically inspired locomotion modes to adapt to diverse terrains and operational scenarios. Each motion type is designed to mimic real snake behavior or other effective movement strategies in nature. These gaits enable the robot to maneuver in tight spaces, climb over obstacles, or self-right when flipped. A summary

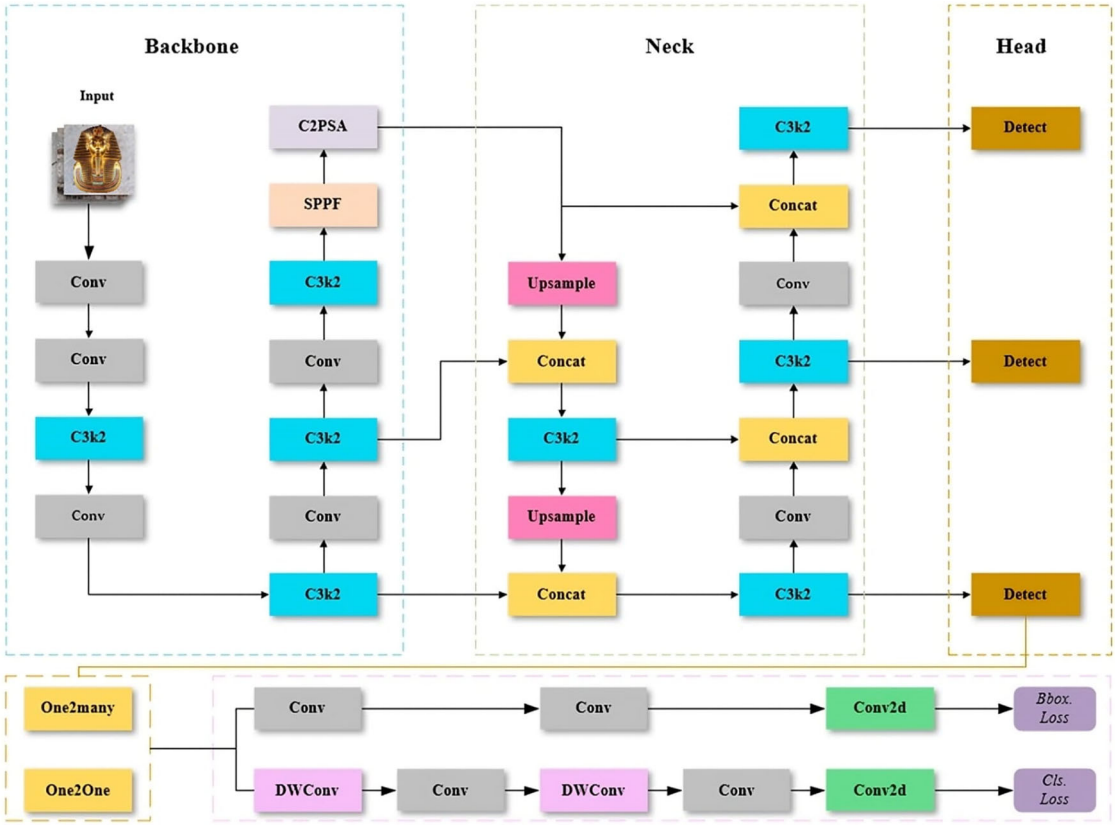

Fig. 12 YOLOv11 architecture

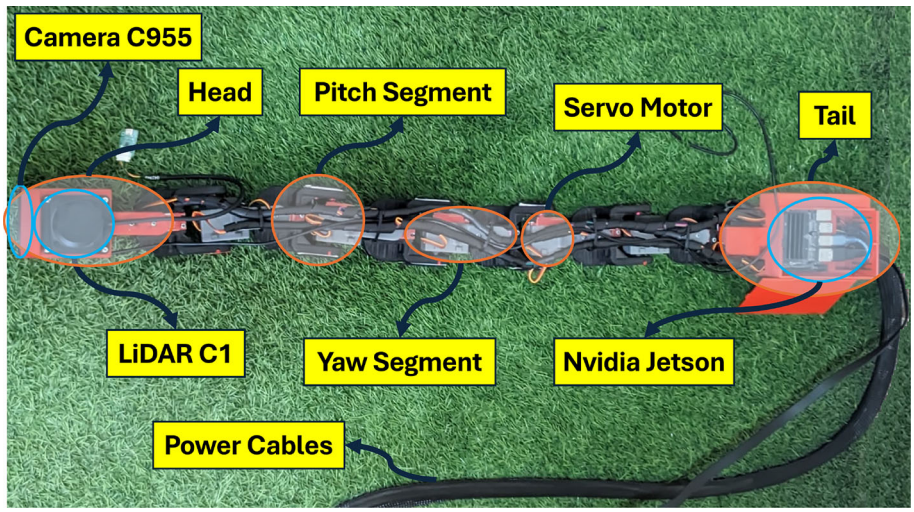

Fig. 13 Fully integrated snake robot with labeled components

of the supported movements, their core principles, and their practical advantages is presented in Table 4

As an example of robot movement in Fig. 14, the cobra positioning gait enables the robot to elevate its anterior modules, mimicking a snake upright stance. This posture enhances the robot's ability to visually scan its surroundings and identify elevated artifacts, such as sculptures or inscriptions. The motion begins from the VIII segment, gradually lifting the body into the characteristic cobra formation through the activation of the X-axis servos. The robot holds this posture momentarily to allow scanning or perception tasks before returning to its nominal stance. This positioning does not result in horizontal displacement but enhances environmental awareness.

The serpentine gait in the XZ plane proved to be the fastest, reaching up to 15 cm/s through vertical oscillations

Table 4 Taxonomy of locomotion gaits and functional capabilities

Movement type	Basic idea	Features/advantages
Serpentine	Generates a traveling sine wave along the body to slither smoothly	Smooth forward/backward motion; useful for self-righting
Inchworm	Sequential contraction and extension of body segments	High precision; effective for climbing
Rectilinear	Lateral shifts using inchworm-like Y-axis actuation	Useful in narrow or confined spaces
Turning	Lifts body via Y-axis and rotates X-axis joints	Orientation adjustment and obstacle avoidance
Safety/Self-righting	Uses X-Y actuators to roll and shift until upright	Autonomous recovery from inverted states
Cobra Positioning	Front of the robot elevates to mimic a cobra stance	Enhances environmental awareness
Obstacle-Aware	Adjusts heading dynamically via sensor feedback	Improves path reliability in cluttered areas

Fig. 14 Execution of the cobra positioning movement from initial rest to elevated scanning posture

that ensured strong traction and rapid travel, whereas the inchworm gait in the XY plane was slower, averaging about 2 cm/s, but achieved very high precision, making it ideal for confined or fragile archeological environments. Our robot reached about 15 cm/s using the XZ-plane serpentine gait, slightly below the nearly 20 cm/s reported in a previous study, mainly because experiments focused on stability and safety in fragile archeological terrain rather than maximum speed. In terms of navigation, the integration of LiDAR with ROS-SLAM allowed the robot to construct accurate occupancy grid maps with minimal drift, even in narrow passages and areas with irregular wall structures. In addition to mapping, the system dynamically adjusted its direction to avoid obstacles, as illustrated in Fig. 15, thereby ensuring reliable trajectory planning and uninterrupted movement. This provided archeologists with precise non-invasive digital records of the exploration site. The robustness of the mapping and obstacle-avoidance framework demonstrates the ability of the robot to adapt to complex archeological environments where traditional surveying methods might be disruptive or impractical. By maintaining localization accuracy, avoiding collisions, and delivering detailed reconstructions, the system forms a critical element of safe autonomous exploration.

4 Results and discussion

This section presents a comprehensive evaluation of the developed autonomous snake robot, validating its design specifications and operational capabilities through both computational modeling and experimental field testing. The main contributions are outlined as follows:

1. **Mathematical and geometrical modeling:** The complete design process of the proposed autonomous snake robot was presented for archeological exploration in con-

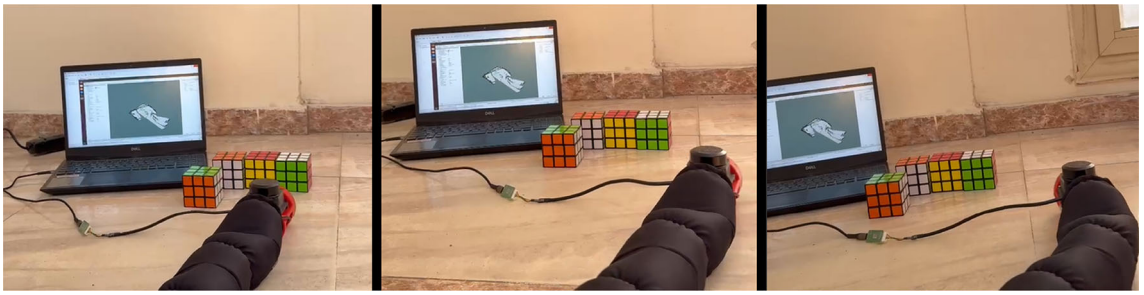

Fig. 15 Snake robot demonstrating obstacle avoidance in front of multiple cube-shaped obstacles

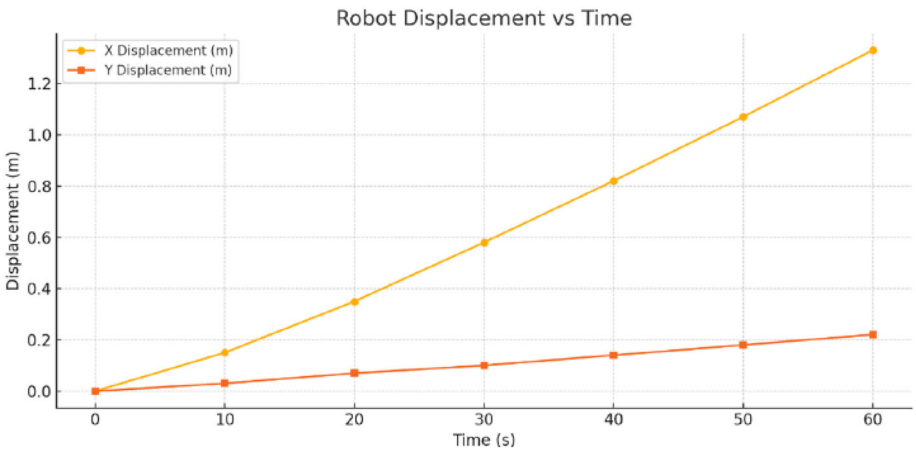

Fig. 16 Snake displacement versus time

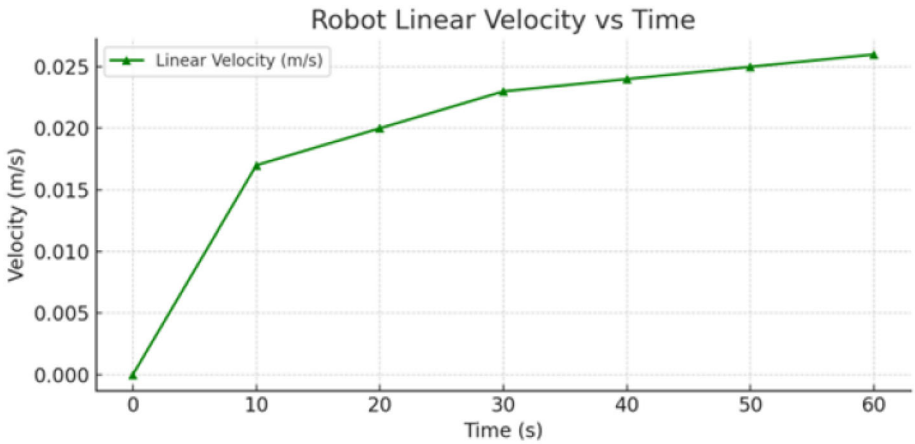

Fig. 17 Snake linear velocity versus time

fined environments. It began with defining functional requirements and selecting a modular architecture, followed by detailed mechanical design with a focus on durability and adaptability. Stress analysis ensured structural integrity, while system modeling and simulation validated the robot expected performance. Key decisions regarding component selection, control strategies, and sensor integration were discussed. A comprehensive kinematic and structural model of the snake robot was created in MATLAB Simscape. The geometrical modeling was customized for incorporation in the Simscape environment with a view to realistically capturing the robot's morphology and motion dynamics. The modeling allowed for design verification and functional validation at an early stage before physical prototyping. As shown in Figs. 16 and 17 the global motion of the snake robot over time. During a 60-second trial, the robot performing lateral undulation (sinusoidal motion) achieved a cumulative displacement of approximately 1.33 m along the X-axis, with a minor lateral drift of around 0.22 m along the Y-axis. The linear velocity gradually increased and stabilized near 0.026 m/s, indicating a consistent traveling wave propagation driving forward movement.

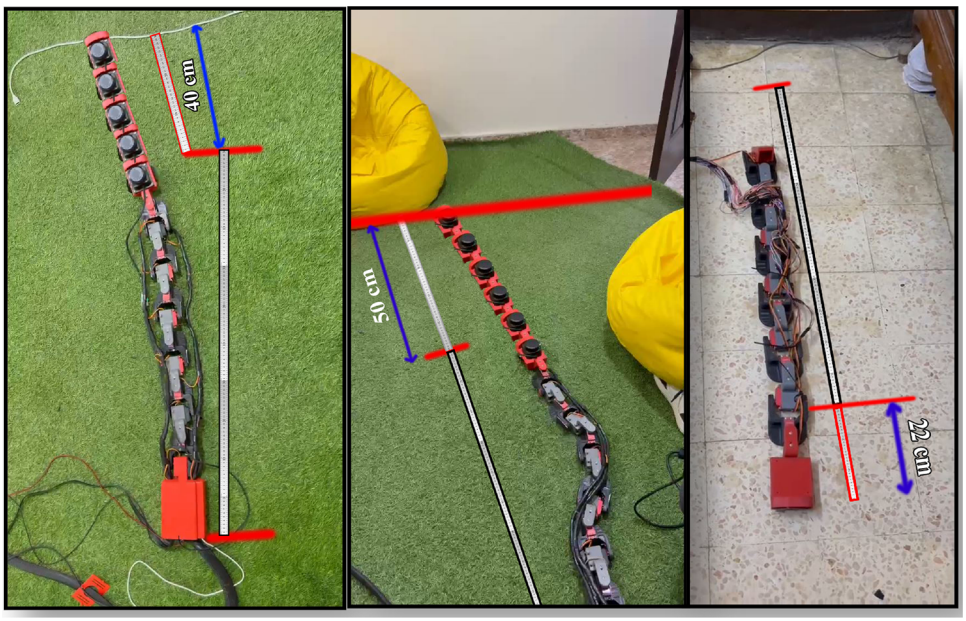

Fig. 18 Locomotion trajectory assessment of the snake robot across various configurations

Table 5 Comparison between simulated and real-world speed performance across five experimental runs

Run	Distance (cm)	Simulated time (s)	Simulated speed (cm/s)	Real time (s)	Real speed (cm/s)	Difference (%)
1	100	250	0.4	274	0.365	−8.75%
2	100	170	0.588	187	0.535	−9.03%
3	100	210	0.476	228	0.438	−7.98%
4	100	240	0.417	261	0.383	−8.18%
5	100	200	0.5	221	0.453	−9.40%
Average Speed			**0.476**		**0.435**	

2. **Integrated sensing and experimental validation:** The experimental realization of the autonomous snake robot, encompassing mechanical fabrication, electrical system integration, and deployment of the control framework were presented. PETG was chosen for 3D printing due to its balance of durability and ease of manufacturing, while a modular design strategy facilitated straightforward assembly and maintenance. The system incorporated a layered PCB structure to manage power distribution, servo motor control, and reliable communication with the Jetson Nano. The control architecture featuring LiDAR-based environmental mapping and coordinated motion via Arduino and PCA9685 was successfully validated The system is coordinated under a ROS-based software architecture, enabling synchronized locomotion control, real time environmental mapping, and easy integration of other sensor modalities. The snake robot was experimentally evaluated to assess its locomotion performance as shown in Fig. 18, mapping capability, and object detection efficiency. Different bio-inspired gaits were tested, each demonstrating specific strengths suitable for archeological missions. The cobra positioning provided a stationary but elevated stance that improved the field of view for scanning inscriptions or detecting obstacles, while the serpentine gait in the XY plane offered stable and smooth forward movement across flat or moderately uneven terrain.

   Table 5 presents a quantitative comparison between the simulated and real-world locomotion speeds across five distinct experimental trials. The results demonstrate a consistent discrepancy, with the physical prototype operating approximately 8.7% slower than the simulation on average, likely due to unmodeled frictional forces and mechanical inefficiencies in the real-world environment.
3. **AI-powered artifact detection:** A deep learning-based perception module with the YOLO architecture for real-time object detection is incorporated. This module allows for the automatic detection and localization of archeological artifacts in unstructured and confined spaces, aiding non-invasive documentation in exploration tasks. Furthermore, onboard perception was enhanced using YOLOv11 deployed on a Jetson Nano, enabling real-time detec-

Fig. 19 Ancient pottery and statue detection

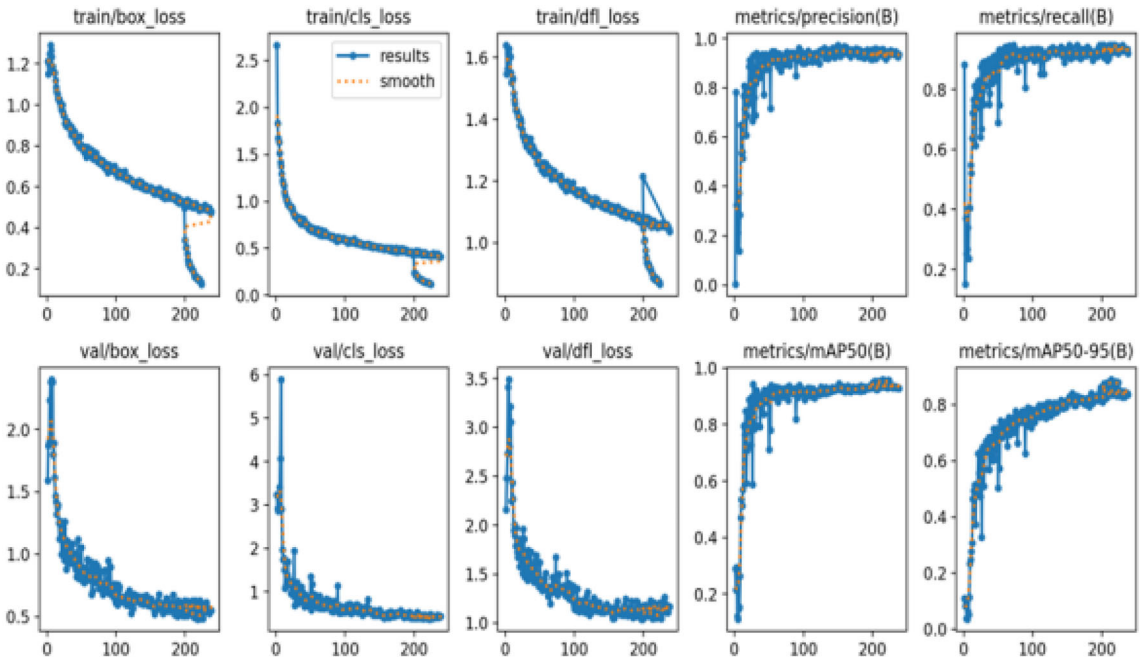

Fig. 20 Accuracy metrics curves

tion of archeological artifacts such as pottery and statues under varying lighting conditions as shown in Fig. 19. The robustness of the detection system confirmed the suitability of the approach for field deployment where conditions are unpredictable. Taken together, the experimental outcomes establish that the developed snake robot combines locomotion versatility for both rapid travel and delicate navigation, reliable ROS-based mapping for safe and autonomous exploration, and AI-driven perception for archeological documentation. This synergy of adaptive gaits, mapping, and onboard intelligence provides a strong foundation for deploying snake robots in real-world archeological missions.

The learning progress of the model was rigorously monitored across 300 epochs, with both training and validation losses examined to ensure stability and generalization. In addition to loss analysis, performance curves for accuracy measures showed the model's strengths and precision. An increasing and consistent trend, showing a reduction in false positives across epochs. Recall: High recall values verified that most relevant artifacts were discovered, limiting false negatives. mAP@0.5: Demonstrated good combination classification and localization accuracy at IoU threshold 0.5. mAP@0.5:0.95: Provided a stricter examination over several IoU thresholds, validating the robustness of YOLOv11 in harsh archeological settings, as shown in Fig. 20.

Collectively, these results indicated that the fine-tuned YOLOv11 model achieved robust training, excellent generalization, and consistent detection performance in complicated archeological contexts.

4. **Limitations and real-world deployment challenges** This platform demonstrates the promise of snake robots as a novel tool for non-invasive archeological exploration, which has the potential to increase access to historical environments that were previously beyond reach. The physical experiments and locomotion tests presented in this study were conducted in controlled laboratory environments. These tests successfully validated the ROS control loop, mapping integrity via Hector SLAM, and YOLOv11 AI inference without risking the physical prototype in hazardous conditions. However, real-world archeological sites present unmodeled environmental factors that differ significantly from our current experimental setup. Challenges such as heavy airborne dust (which can interfere with LiDAR accuracy), loose rubble and uneven ground (which introduce unexpected slip dynamics), and extreme low-lighting conditions will directly impact sensor reliability and locomotion efficiency. Addressing these specific real-world deployment challenges will be the primary focus of future field-testing phases.

5 Conclusion

This article presented the complete design process of an autonomous snake robot for archeological exploration in confined environments. Firstly, mathematical modeling of the snake robot has been performed using MATLAB Simscape, enabling precise simulation and analysis of its mechanical and electrical components. The mathematical modeling results informed the selection of actuators, and the mechanical design was subsequently developed and validated using ANSYS software and PETG material was utilized for 3D printing the designed parts. Secondly, a custom printed circuit board (PCB) was designed and fabricated, integrating all the wiring into a single board, thereby enhancing system reliability and efficiently distributing power to the motors for precise control of the robot's movements. Thirdly, a robust control system was developed for the robot, integrating LiDAR, NVIDIA Jetson, Arduino, and PCA9685, and leveraging the Robot Operating System (ROS) to enable intelligent movement, real-time mapping, and precise localization, resulting in a flexible and expandable system. Finally, an AI-powered object detection system utilizing YOLO technology was developed and added to the robot, enabling real-time identification and localization of archeological artifacts from live camera feeds. Overall, this work illustrates how integrating bio-inspired locomotion with modern perception frameworks can yield robotic platforms capable of safe, non-invasive exploration in sensitive environments. While the current prototype successfully demonstrates computationally autonomous navigation and real-time mapping, it remains a tethered laboratory proof-of-concept due to the high power demands of the serial actuators. Future work will focus on transitioning the system from tethered external power to an onboard, high-discharge battery architecture to achieve full physical autonomy. Subsequent phases will involve extensive field deployment in real heritage sites, energy optimization for long-duration missions, and the incorporation of tactile sensing to further enhance body-environment interaction.

Supplementary Information The online version contains supplementary material available at https://doi.org/10.1007/s40435-026-02134-w.

Acknowledgements This research was funded by the Academy of Scientific Research and Technology (ASRT), Egypt, under Grant Number 105.

Author Contributions Conceptualization, Mohamed Shehata. And Mohamed Eltaher, methodology, Ahmed Elsayed and Ahmed Youns; software, Ibrahim Saeed; validation, Ahmed Youns; formal analysis, Ahmed Elsayed; writing—original draft preparation, Ahmed Elsayed, Ahmed Youns and Ibrahim Saeed; writing—review and editing, Mohamed Shehata; visualization, Mohamed Eltaher; supervision, Mohamed Shehata. All authors have read and agreed to the published version of the manuscript.

Funding Open access funding provided by The Science, Technology & Innovation Funding Authority (STDF) in cooperation with The Egyptian Knowledge Bank (EKB).

Data Availability The datasets generated during and/or analyzed during the current study are available from the corresponding author on reasonable request

Code Availability The code used to support the findings of this study is available from the corresponding author upon reasonable request.

Declarations

Conflict of interest The authors declare no conflict of interest.

References

1. Tom L, Cyprien C, Dossou P-E, Gaspard L (2023) Towards a robotic intervention for on land archaeological fieldwork in prehistoric sites. In: International conference on flexible automation and intelligent manufacturing, pp. 79–90. Springer, Cham

2. Hopkins JK, Spranklin BW, Gupta SK (2009) A survey of snake-inspired robot designs. Bioinspiration Biomimet 4(2):021001
3. Floreano D, Mattiussi C (2008) Bio-inspired Artificial Intelligence: Theories, Methods, and Technologies. MIT press, Cambridge
4. Liljebäck P, Pettersen KY, Stavdahl Ø, Gravdahl JT (2012) Snake Robots: Modelling, Mechatronics, and Control. Advances in Industrial Control. Springer, London
5. Li D, Zhang B, Xiu Y, Deng H, Zhang M, Tong W, Law R, Zhu G, Wu EQ, Zhu L (2022) Snake robots play an important role in social services and military needs. Innov 3(6)
6. Seetohul J, Shafiee M (2022) Snake robots for surgical applications: A review. Robotics 11(3):57
7. Richardson R, Whitehead S, Ng T, Hawass Z, Pickering A, Rhodes S, Grieve R, Hildred A, Nagendran A, Liu J et al (2013) The "djedi" robot exploration of the southern shaft of the queens chamber in the great pyramid of Giza, Egypt. J Field Robot 30(3):323–348
8. Kabir H, Tham M, Chang Y (2023) Internet of robotic things for mobile robots: Concepts, technologies, challenges, applications, and future directions. Digital Commun Netw 9(6):1265–1290
9. Marvi H, Cook J, Streator J, Hu D (2016) Snakes move their scales to increase friction. Biotribology 5
10. Wang J, Zhu X, Tie F, Zhao T, Xu X (2009) Design of a modular robotic system for archaeological exploration. In: 2009 IEEE international conference on robotics and automation, pp. 1435–1440 . IEEE
11. Shao Q, Xia Q, Lin Z, Dong X, An X, Zhao H, Li Z, Liu X-J, Dong W, Zhao H (2025) Unearthing the history with a-rhex: Leveraging articulated hexapod robots for archeological pre-exploration. J Field Robot 42(1):206–218
12. Fu Q (2023) Snake and snake robot locomotion in complex, 3-d terrain. Doctoral dissertation, Johns Hopkins University
13. Coad M, Blumenschein L, Cutler S, Zepeda J, Naclerio N, El-Hussieny H, Mehmood U, Ryu J, Hawkes E, Okamura A (2019) Vine robots: Design, teleoperation, and deployment for navigation and exploration. arXiv preprint arXiv:1903.00069
14. Li G, Waldum HB, Grindvik MO, Jørundl RS, Zhang H (2020) Development of a vision-based target exploration system for snake-like robots in structured environments. Int J Adv Rob Syst 17(4):1729881420936141
15. Alkendi Y, Seneviratne L, Zweiri Y (2021) State of the art in vision-based localization techniques for autonomous navigation systems. IEEE Access 9:76847–76874
16. Siciliano B, Sciavicco L, Villani L, Oriolo G (2010) Robotics: Modelling, Planning and Control. Springer, London
17. Kelly A (2013) Mobile Robotics: Mathematics, Models, and Methods. Cambridge University Press, Cambridge
18. Shehata M, Salem ME (2025) The importance of educating dynamics for design techniques to improve the scientific level of graduate engineering students. Benha J Eng Sci Technol 2(1):1–8
19. Elshami M, Shehata M, Bai Q, Zhao X (2021) Multibody dynamics modeling of delta robot with experimental validation. In: International symposium on multibody systems and mechatronics, pp. 94–102 . Springer
20. Ito K, Murai R (2008) Snake like robot for rescue operations-proposal of a simple adaptive mechanism designed for ease of use. Adv Robot 22(6–7):771–785
21. Wei W, Yu JX, Lin WH, Mai RS, Chen CX, He ZY, Li Z (2014) Structure design of climbing snake-like robot for detection of cable-stayed bridge. Appl Mech Mater 598:610–618
22. Bai Q, Shehata M, Nada A (2020) Efficient modeling procedure of novel grating tiling device using multibody system approach. In: International symposium on multibody systems and mechatronics, pp. 168–176 . Springer
23. Bai Q, Shehata M, Nada A (2022) Review study of using Euler angles and Euler parameters in multibody modeling of spatial holonomic and non-holonomic systems. Int J Dynam Control 10(5):1707–1725
24. Jeevanantham P, Stephen JDG (2018) Dynamic optimization of snake robot with environment detection and analysis. In: IOP conference series: materials science and engineering, vol. 402, p. 012019 . IOP Publishing
25. Grabec I (2002) Control of a creeping snake-like robot. In: Proceedings of the 7th international workshop on advanced motion control, pp. 526–531
26. Kano T, Date H, Ishiguro A (2014) Simple decentralized control scheme can reproduce versatile gait patterns of snakes. In: Proceedings of the international symposium on nonlinear theory and its applications (NOLTA), pp. 3–20
27. Guyot A, Lennon M, Lorho T, Hubert-Moy L (2021) Combined detection and segmentation of archeological structures from lidar data using a deep learning approach. J Comput Appl Archaeol 4(1):1–19
28. Chen Y, Zhang A, Shi J, Gao F, Guo J, Wang R (2025) Paint loss detection and segmentation based on yolo: An improved model for ancient murals and color paintings. Heritage 8(4):136
29. Olivier M, Verschoof-van Der Vaart W (2021) Implementing state-of-the-art deep learning approaches for archaeological object detection in remotely-sensed data: The results of cross-domain collaboration. J Comput Appl Archaeol 4(1)
30. Cardarelli L (2025) Pypotterylens: An open-source deep learning framework for automated digitisation of archaeological pottery documentation. Digital Applications in Archaeology and Cultural Heritage, 00452